TRENDS IN SCIENCES 2026; 23(12): 13774
https://doi.org/10.48048/tis.2026.13774 RESEARCH ARTICLE

Antibiofilm Effect of Curcumin-Derived Carbon Dots against *Pseudomonas aeruginosa* on the Urinary Catheter

Dewi Santosaningsih[1,2,*], Keneysha Naomi Mataniari[3], Dian Nugrahenny[4], Azzania Fibriani[5,6], Arum Sinda Santika[7,8], Fitri Aulia Permatasari[6,7] and Ferry Iskandar[6,7]

[1]*Department of Clinical Microbiology, Faculty of Medicine, Universitas Brawijaya, Malang, Indonesia*
[2]*Department of Clinical Microbiology, Dr. Saiful Anwar Hospital, Malang, Indonesia*
[3]*Master Program in Biomedical Sciences, Faculty of Medicine, Universitas Brawijaya, Malang, Indonesia*
[4]*Department of Pharmacology, Faculty of Medicine, Universitas Brawijaya, Malang, Indonesia*
[5]*School of Life Sciences and Technology, Institut Teknologi Bandung, Bandung, Indonesia*
[6]*Research Center for Nanoscience and Nanotechnology, Institut Teknologi Bandung, Bandung, Indonesia*
[7]*Department of Physics, Faculty of Mathematics and Natural Sciences, Institut Teknologi Bandung, Bandung, Indonesia*
[8]*Department of Physics, Universitas Pembangunan Nasional Veteran Jawa Timur, Surabaya, Indonesia*

([*]Corresponding author's e-mail: dewi.santosa@ub.ac.id)

Received: 7 March 2026, Revised: 16 May 2026, Accepted: 26 May 2026, Published: 25 July 2026

Abstract

Pseudomonas aeruginosa (*P. aeruginosa*) is a major opportunistic pathogen in patients with prolonged urinary catheterization. Its intrinsic multidrug resistance and robust biofilm-forming capacity on catheter surfaces contribute to persistent colonization and recurrent catheter-associated urinary tract infections. Although *Curcuma longa*–derived curcumin exhibits antibiofilm activity, its clinical utility is limited by poor bioavailability. Carbon dots (CDs) have emerged as effective platforms for enhancing antimicrobial delivery. However, study on the effect of antibiofilm of curcumin-derived carbon dots (cur-CDs), particularly on medical devices, is limited. This study aimed to evaluate the antibiofilm efficacy of cur-CDs against *P. aeruginosa* ATCC 9027 biofilms formed on urinary catheter surfaces. Cur-CDs were characterized using UV–visible spectroscopy, Fourier-Transform Infrared Spectroscopy, photoluminescence spectroscopy, and Transmission Electron Microscopy. Biofilm inhibition was assessed using a tissue culture plate assay at cur-CDs concentrations ranging from 5, 10, 20, 30, 40 and 50 µg/mL. Biofilm biomass was quantified spectrophotometrically, viable biofilm-associated bacteria were enumerated by colony-forming unit analysis, and biofilm architecture was examined by field emission scanning electron microscopy. Cur-CDs exhibited a significant, concentration-dependent antibiofilm effect, resulting in marked reductions in biofilm biomass ($p < 0.0001$) and viable bacterial counts ($p = 0.001$). This enhanced antibiofilm activity may be attributed to the nanoscale properties of cur-CDs, which potentially improve curcumin stability and facilitate interactions with bacterial membranes and the biofilm matrix. Overall, cur-CDs effectively inhibit *P. aeruginosa* biofilm formation on urinary catheter surfaces and support their potential application as an antibiofilm strategy for mitigating catheter-associated urinary tract infections.

Keywords: Biofilms, Carbon dots, Catheter-associated urinary tract infection, *Curcumin*, Nanoparticles, *Pseudomonas aeruginosa*, Urinary catheters

Introduction

Catheter-Associated Urinary Tract Infections (CAUTI) are one of the most prevalent hospital-acquired infections and are associated with serious complications, including cystitis, pyelonephritis, renal

stone, and septicaemia [1,2]. WHO reported that 7% of patients at least acquired one HAIs during hospitalization in high income countries and 15% in low- and middle- income countries [3]. Current point prevalence survey conducted in 2022 - 2023 across 1,250 acute care hospitals in 28 countries of the European Union and European Economic Area (EU/EEA) demonstrated that the most common type of HAI were respiratory tract infections (29.3%) followed by urinary tract infections (19.2%) [4]. Among urinary tract infections acquired in the hospital, 75% are CAUTI [5]. The complications associated with CAUTI contribute to prolonged hospital stays, antibiotic overuse, and increased healthcare cost and mortality [3,6,7].

The use of indwelling catheter contributes to the CAUTI development. CAUTI incidence per 1,000 catheter-days remains elevated among critically ill patients with ICU stays exceeding 48 hours. In a cohort of 54 ICU patients, *Pseudomonas aeruginosa* (*P. aeruginosa*) was identified as the predominant pathogen associated with CAUTI [2]. Antibiotics are the mainstay of CAUTI treatment, however, infections caused by *P. aeruginosa* are frequently difficult to eradicate because of biofilm formation [7,8]. Abiotic surface of the catheter is subject to biofilm formation. Biofilm-embedded bacteria demonstrate up to a 10 - 1,000-fold increase in antibiotic tolerance compared with planktonic cells, driven by impaired antimicrobial diffusion through the polysaccharide matrix and biofilm-associated shifts in metabolism and protein expression [7,9].

Curcuma longa represents one of Indonesia's biodiversity resources and has long been utilized in traditional medicine due to its antimicrobial activity [10]. Curcumin is the main bioactive compound of *Curcuma longa* and largely accounts for its antibacterial properties. Despite limitations such as poor water solubility, low bioavailability, and suboptimal pharmacokinetic characteristics, previous studies have demonstrated that curcumin possesses potent antimicrobial and antibiofilm activities, primarily through the disruption of bacterial quorum sensing (QS) systems [11,12].

Carbon dots (CDs) are spherical nanomaterials with diameters below 10 nm and have demonstrated considerable promise across diverse applications, including biomedical. In antibiofilm applications, CDs have attracted particular interest due to their nanoscale dimensions and physicochemical properties, which enable efficient penetration of the biofilm extracellular polymeric matrix and help overcome the diffusion limitations commonly encountered with conventional antimicrobial agents [13].

Previous studies on cur-CDs have mainly focused on their antibacterial effects against planktonic cells. Studies investigating the antibiofilm effects of cur-CDs, particularly on medical devices, remain limited [14]. To our knowledge, only one study has reported the antibiofilm activity of curcumin-derived carbon dots (cur-CDs) against biofilm-producing *Enterococcus faecium* [15]. The antibiofilm effects of cur-CDs against *P. aeruginosa*, particularly on urinary catheters, remain unclear. Therefore, this study aimed to assess the antibiofilm activity of cur-CDs against *P. aeruginosa* on urinary catheters.

Materials and methods

Urinary catheters pieces preparation

Urinary catheter packages (Latex Foley Catheter, ONEHEALTH Medical, Indonesia) were opened inside a biological safety cabinet. The catheters were aseptically cut into approximately 0.5-cm segment using a sterile scalpel. Each sterile catheter segment was then placed into an individual well of a tissue culture plate for subsequent experiments [16].

Bacterial isolate

P. aeruginosa ATCC 9027 was used in this study. Colonies from fresh agar plates were inoculated into 5 mL of trypticase soy broth (Oxoid, Basingstoke, UK) and incubated at 37 °C for 24 h. The bacterial suspension was then adjusted spectrophotometrically to approximately 10^8 CFU/mL and used to initiate biofilm formation on urinary catheter segments.

Cur-CDs preparation

Cur-CDs were synthesized using a solvothermal approach as previously described [17,18]. Briefly, citric acid (0.3 mol; Sigma Aldrich, USA) and urea (1.5 mol; Sigma Aldrich, USA) were dissolved in deionized water under continuous stirring at room temperature. Separately, curcumin (1 mmol $C_{21}H_{20}O_6$; Combiphar, Indonesia) was dispersed in ethanol at ambient

conditions. The curcumin suspension was subsequently combined with the aqueous precursor mixture and maintained at 60 °C for 30 min. The resulting solution was transferred into a Teflon-lined autoclave and heated at 200 °C for 5 h. After cooling, the reaction mixture was clarified by centrifugation and further purified using a 0.22 μm regenerated cellulose membrane filter. The purified product was freeze-dried to obtain cur-CD powder. Both curcumin and cur-CD powders were reconstituted in dimethyl sulfoxide and sterile distilled water, respectively. Stock solutions were protected from light and stored at −20 °C [19].

Cur-CDs characterization

The physicochemical and optical properties of the synthesized cur-CDs were characterized using UV–visible spectrophotometry, UV–Vis Genesys 150 (Thermo-fisher scientific, USA)), photoluminescence (PL) spectroscopy, Cary eclipse fluorescence Spectrophotometer (Agilent, USA), Fourier-Transform Infrared (FTIR) spectroscopy (Shimadzu, Japan) and Transmission Electron Microscopy (TEM) (HR-TEM, Tecnai G2 20S-Twin). UV–Vis absorption spectra were recorded over the range of 200 - 800 nm using sterile distilled water as a blank to identify characteristic electronic transitions associated with CD formation. PL measurements were performed using a fluorescence spectrophotometer by exciting aqueous cur-CDs suspensions at selected wavelengths and collecting emission spectra over an appropriate range to evaluate excitation-dependent fluorescence behavior. FTIR analysis was conducted to identify surface functional groups and chemical bonding, with spectra acquired over the range of 4,000 - 400 cm^{-1}. Morphology and particle size were examined by TEM; a drop of diluted cur-CD suspension was deposited onto carbon-coated copper grids, air-dried, and imaged to determine particle shape and size distribution [18].

Biofilm inhibition assay of cur-CDs against *P. aeruginosa* on the urinary catheter

Biofilm formation by *P. aeruginosa* ATCC 9027 on urinary catheter pieces was assessed using the tissue culture plate method. The antibiofilm effects of cur-CDs were evaluated against early-stage biofilms using a 2-phase incubation protocol. Sterile catheter pieces were placed into individual wells of a 24-well flat-bottom polystyrene plates (Biologix Europe GmbH, Hallbergmoos, Germany). Each well contained 200 μL of bacterial suspension 10^8 CFU/mL and 200 μL of trypticase soy broth supplemented with glucose. Wells containing uninoculated medium served as negative controls to confirm sterility. Following incubation at 37 °C for 8 h, the supernatant was carefully removed and wells were rinsed twice with 200 μL phosphate-buffered saline (PBS; pH 7.2). Pieces of urinary catheter were subsequently transferred to fresh wells containing 200 μL of glucose-free trypticase soy broth with the designated treatments (**Table 1**) [20], and plates were incubated for an additional 24 h at 37 °C.

After the second incubation, wells were washed twice with PBS and incubated at 37 °C for one hour. Biofilms were stained with 200 μL of 0.1% crystal violet for 10 min, followed by 2 rinses with deionized water to remove excess dye. After drying, bound stain was solubilized with 200 μL of 33% glacial acetic acid. Biofilm biomass was quantified by measuring optical density at 570 nm using a microplate reader (Bio-Rad, Hercules, CA, USA). All experiments were conducted in quadruplicate technically. Biofilm formation was categorized according to optical density cutoff value (ODc). The ODc was defined as average optical density (OD) of negative control + (3x standard deviations of the negative controls). Samples were categorized as non-biofilm producers when $OD \leq ODc$, weak biofilm producers when $ODc < OD \leq 2 \times ODc$, moderate biofilm producers when $2 \times ODc < OD \leq 4 \times ODc$, and strong biofilm producers when $OD > 4 \times ODc$ [21]. Inhibition percentages were calculated using the formula as follows: % inhibition = 100 − [(OD570 sample/OD570 untreated control)×100] [22].

Table 1 The biofilm inhibition assay of cur-CDs against *P. aeruginosa* biofilm.

Group	Treatment
1	*P. aeruginosa* ATCC 9027 (untreated – positive control)
2	*P. aeruginosa* ATCC 9027 + cur-CDs 5 μg/mL
3	*P. aeruginosa* ATCC 9027 + cur-CDs 10 μg/mL
4	*P. aeruginosa* ATCC 9027 + cur-CDs 20 μg/mL
5	*P. aeruginosa* ATCC 9027 + cur-CDs 30 μg/mL
6	*P. aeruginosa* ATCC 9027 + cur-CDs 40 μg/mL
7	*P. aeruginosa* ATCC 9027 + cur-CDs 50 μg/mL

Quantification of bacterial biofilms

Bacterial biofilms were quantified as previously described [23]. In brief, bacterial biofilms were detached from urinary catheter pieces by sequential vortexing and sonication. The sonicate was concentrated by centrifugation at 3,100×g for 10 min, and the pellet was resuspended in 1 mL phosphate-buffered saline. The recovered sonicate, along with its serial dilutions, was inoculated onto LB agar plates using a 20-μL drop-plating technique performed in triplicate, followed by incubation at 37 °C for 14 - 18 h. Colony counts were recorded for each dilution, and biofilm-associated bacterial density was calculated as CFU/cm using the equation: CFU/cm = (mean colony count per dilution)×50×dilution factor.

Field emission scanning electron microscopy (FESEM)

FESEM sample preparation was conducted according to the previously described [24]. Briefly, culture supernatants were removed, and urinary catheter pieces were rinsed twice with sterile 1% phosphate-buffered saline (Merck, USA), fixed in 2.5% glutaraldehyde for 2 h, and dehydrated through a graded ethanol series. The samples were air-dried overnight, gold-coated, and examined using a HITACHI REGULUS 8220 FESEM at the Laboratory of Chemical Instrumentation, Faculty of Science and Data Analytics, Institut Teknologi Sepuluh Nopember, Surabaya, Indonesia.

Statistical analysis

Biofilm biomass data were analyzed using one-way analysis of variance (ANOVA) followed by Tukey's multiple comparison test after confirming normal distribution and homogeneity of variance among groups. Data are presented as mean ± standard deviation (SD), and statistical significance was defined at $p < 0.05$. In contrast, viable bacterial count (CFU/cm) data did not meet the normality assumption, as the control (C) and cur-CDs 40 μg/mL groups showed non-normal data distribution. Therefore, statistical analysis for bacterial viability was performed using the non-parametric Kruskal-Wallis test followed by Dunn's multiple comparison post hoc test. Data are presented as mean ± SD, with statistical significance set at $p < 0.05$.

Results and discussion

cur-CDs properties

The structural and optical properties of the cur-CDs was summarized in **Figure 1**. The transmission electron microscopy (TEM) was used to evaluate the particle structure and size distribution of cur-CDs, as presented in **Figure 1(a)**. The TEM image reveals that sample exhibit well-dispersed, quasi-spherical without noticeable agglomeration, with an average diameter of 7.1 ± 1.3 nm, indicating a narrow size distribution and homogenous morphology. The relatively uniform distribution and absence of large aggregates indicate good colloidal stability [17]. The UV-Vis spectrum, as shown in **Figure 1(b)**, exhibit 2 peak absorption band centered at 278 and 338 nm, which can be assigned to π–π* transition of sp^2-conjugated C=C domain and n–π* transition associated with carbonyl-related functionalities (e.g., C=O), respectively. This feature is commonly observed with carbon dots systems and indicative of a conjugated carbon core decorated with surface states [25]. The PL excitation-dependent emission map (**Figure 1(c)**) presents a broad, excitation-dependent emission behavior, with the dominant

emission residing in the range 400 - 500 nm window under excitation spanning approximately 250 - 450 nm. Such excitation-dependent luminescence suggests a distribution of emissive traps/defect states and heterogeneous surface energy levels, rather than a single molecular, which is typical for CDs with mixed core/surface contributions [25]. FTIR analysis (**Figure 1(d)**) Further confirms the presence of abundant surface functional groups, a broad band in the ~3,200 - 3,500 cm^{-1} region corresponds to overlapping O–H/N–H stretching vibrations, while bands in the ~1,700 - 1,500 cm^{-1} region are attributable to C=O and/or C=N vibrations together with contributions from C=C stretching of aromatic/sp^2 carbon. Additional absorptions in the ~1,300 - 1,000 cm^{-1} range are consistent with C–N stretching, corroborating nitrogen/oxygen-containing surface functionalities. These results confirm the successful synthesis of cur-CDs with characteristic optical properties, surface chemistry, and nanoscale morphology.

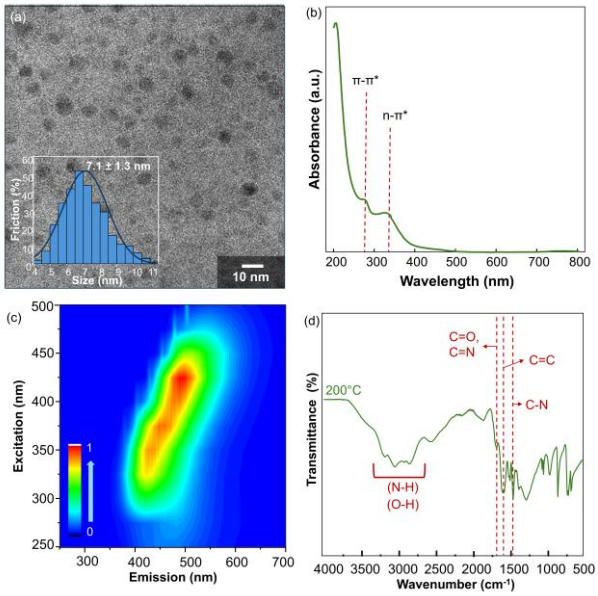


Figure 1 Characterization of cur-CDs. (a) TEM image and inset size distribution, (b) UV-vis absorption spectra, (c) PL Mapping, and (d) FTIR spectra.

Biofilm inhibition activities of cur-CDs against *P. aeruginosa* on the urinary catheter

The effect of cur-CDs on biofilm formation by *P. aeruginosa* on urinary catheter pieces was evaluated based on optical density values. **Figure 2** shows that the biofilm biomass on urinary catheter pieces decreased with increasing cur-CDs concentration, which is consistent with the optical density values presented in **Table 2** and **Figure 3(A)**.

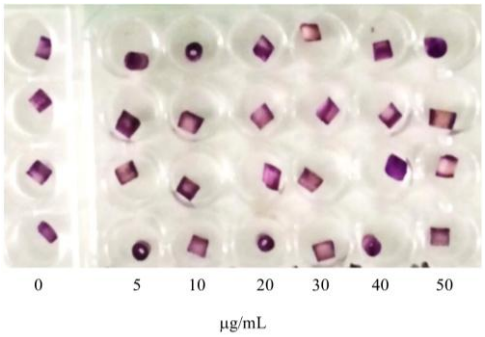


Figure 2 Detection of biofilm formation of *P. aeruginosa* on urinary catheter pieces after exposure of cur-CDs from 5 to 50 μg/mL. Four replicates are shown in each column.

Table 2 Production of biomass biofilm of *P. aeruginosa* ATCC 9027 on the urinary catheter based on optical density values.

Group	Replication	OD	Mean ± SD	Interpretation
Untreated (positive control)	1	2.955	2.946 ± 0.052[a]	Strong biofilm formation
	2	2.918		
	3	3.016		
	4	2.895		
cur-CDs 5 µg/mL	1	2.958	2.115 ± 0.620[b]	Strong biofilm formation
	2	1.463		
	3	2.049		
	4	1.992		
cur-CDs 10 µg/mL	1	1.979	1.603 ± 0.272[b-c]	Strong biofilm formation
	2	1.534		
	3	1.329		
	4	1.572		
cur-CDs 20 µg/mL	1	1.466	1.317 ± 0.199[c]	Moderate biofilm formation
	2	1.046		
	3	1.469		
	4	1.290		
cur-CDs 30 µg/mL	1	1.428	1.431 ± 0.216[b-c]	Moderate biofilm formation
	2	1.148		
	3	1.476		
	4	1.674		
cur-CDs 40 µg/mL	1	1.623	1.518 ± 0.440[b-c]	Moderate biofilm formation
	2	0.956		
	3	1.474		
	4	2.021		
cur-CDs 50 µg/mL	1	1.286	1.416 ± 0.150[b-c]	Moderate biofilm formation
	2	1.501		
	3	1.294		
	4	1.585		

[a], [b], [b-c], and c notifications according to the post hoc test: Value with different superscript letters are significantly different ($p < 0.05$); groups sharing at least one common letter are not significantly different.

Table 3 Quantification of bacterial biofilm of *P. aeruginosa* on the urinary catheter pieces.

Group	Replication	CFU/cm (×10^3)	Mean (×10^3) ± SD (×10^3)
Untreated (positive control)	1	1,272,104	1,400,000 ± 254,352[a]
	2	1,272,056	
	3	1,780,800	
	4	1,272,126	

Group	Replication	CFU/cm (×10³)	Mean (×10³) ± SD (×10³)
cur-CDs 5 µg/mL	1	310,000	660,950 ± 467,955[a-b]
	2	890,400	
	3	235,000	
	4	1,208,400	
cur-CDs 10 µg/mL	1	63,600	228,960 ± 115,184[a-c]
	2	267,120	
	3	254,400	
	4	330,720	
cur-CDs 20 µg/mL	1	133,560	173,310 ± 64,729[a-c]
	2	127,200	
	3	165,360	
	4	267,120	
cur-CDs 30 µg/mL	1	127,200	119,254 ± 60,848[b-c]
	2	120,840	
	3	114,497	
	4	114,480	
cur-CDs 40 µg/mL	1	45,000	175,020 ± 87,351[a-c]
	2	228,960	
	3	222,600	
	4	203,520	
cur-CDs 50 µg/mL	1	2,035.2	2,146 ± 276[c]
	2	2,544.0	
	3	1,908.0	
	4	2,098.8	

[a], [a-b], [a-c], [b-c], and c notifications according to the post hoc test: value with different superscript letters are significantly different ($p < 0.05$); groups sharing at least one common letter are not significantly different.

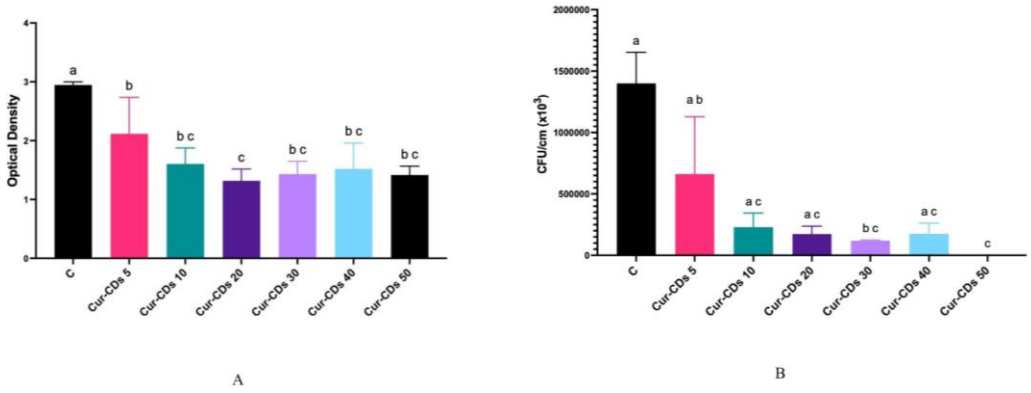


Figure 3 Biomass biofilm (A) and bacterial biofilm (B) of *P. aeruginosa* on urinary catheter pieces. C: untreated *P. aeruginosa* ATCC 9027; Cur-CDs 5, 10, 20, 30, 40 and 50: *P. aeruginosa* ATCC 9027 treated with Cur-CDs 5, 10, 20, 30, 40 and 50 µg/mL. Different notations indicate significant differences.

Figure 3(A) demonstrates that the untreated group (positive control) exhibited the highest biofilm biomass (OD= 2.946 ± 0.053), confirming strong biofilm formation. Treatment with cur-CDs significantly reduced biofilm formation at all tested concentrations compared with the control. The most pronounced inhibition was observed at 20 µg/mL (OD = 1.318 ± 0.200; $p < 0.0001$), followed by 30, 40, and 50 µg/mL, all of which showed comparable antibiofilm activity. Although biofilm biomass generally decreased with increasing cur-CDs concentration, no significant differences were observed among most treatment groups ($p > 0.05$), except between 5 and 20 µg/mL ($p = 0.0356$). These findings demonstrate the potent antibiofilm activity of cur-CDs, with 20 µg/mL representing the optimal effective concentration.

Figure 3B shows that the untreated group exhibited the highest bacterial load (1.40×10^6 CFU/cm³), confirming extensive biofilm-associated bacterial growth. Treatment with cur-CDs markedly reduced viable bacterial counts across all concentrations, with the strongest reduction observed at 50 µg/mL ($2{,}146\times10^3$ CFU/cm), followed by 30 µg/mL ($119{,}254\times10^3$ CFU/cm). Dunn's post hoc analysis demonstrated significant reductions in bacterial burden for cur-CDs 30 µg/mL ($p = 0.0444$) and 50 µg/mL ($p = 0.0008$) compared with the untreated group. Notably, the 50 µg/mL group formed a distinct statistical subset in the compact letter display analysis, indicating superior antibacterial efficacy. These findings highlight the potent dose-dependent antibiofilm and antibacterial activity of cur-CDs, particularly at higher concentrations.

FESEM images (**Figure 4**) illustrate the surface morphology and biofilm architecture of *P. aeruginosa* on urinary catheter pieces. In the untreated group (A), dense and continuous biofilm coverage is observed, characterized by multilayered aggregates of rod-shaped bacterial cells embedded in an abundant extracellular matrix. Following treatment groups (B–G), disruption of the biofilm structure is evident. The treated samples show reduced bacterial aggregation, decreased extracellular matrix coverage, and the appearance of scattered and partially detached bacterial cells. At higher treatment conditions, the biofilm architecture appears thinner and less compact. Individual bacterial cells are more clearly distinguishable, suggesting impaired cell-to-cell adhesion and biofilm integrity.

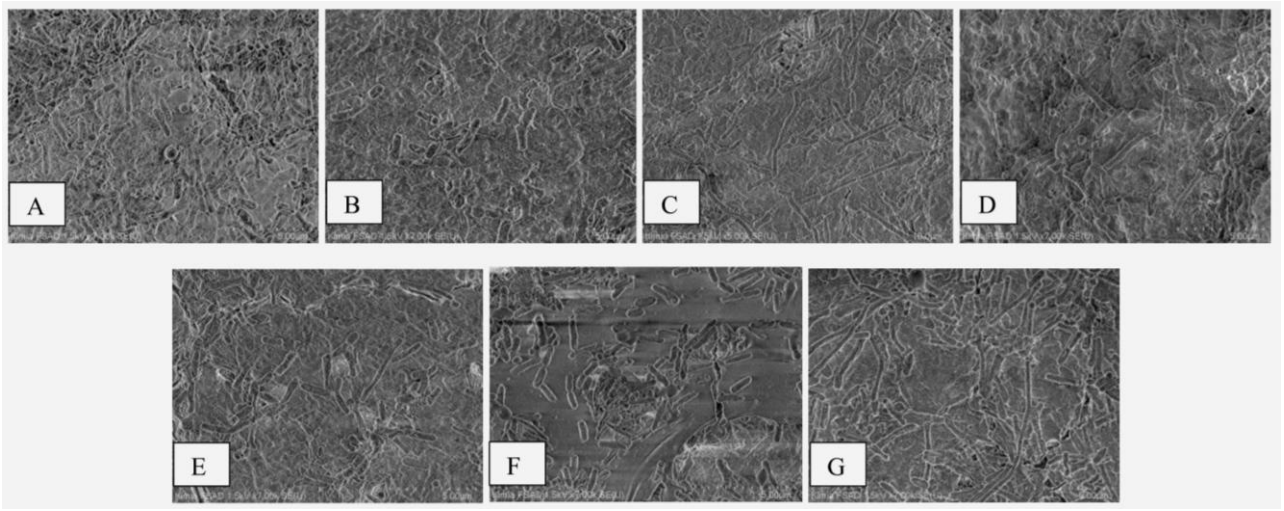


Figure 4 Field emission scanning microscopy of *P. aeruginosa* biofilm formation on the urinary catheter surfaces. A= Untreated group; B = cur-CDs 5 µg/mL; C = cur-CDs 10 µg/mL; D = cur-CDs 20 µg/mL; E = cur-CDs 30 µg/mL; F = cur-CDs 40 µg/mL; G = cur-CDs 50 µg/mL. The magnification was 7,000×.

CAUTI is a leading hospital-acquired infection, responsible for nearly 40% of cases and second only to respiratory infections in incidence. Bacterial biofilm formation on indwelling urethral catheters has been identified as a major factor contributing to both the high

incidence and the therapeutic difficulty of CAUTI [26-28].

P. aeruginosa is a major pathogen causing CAUTI, particularly due to its ability to form antibiotic-resistant biofilms on the surface of urinary catheters. Considerable efforts have been directed toward the development of strategies to treat and eradicate biofilms, particularly those formed by *P. aeruginosa* [13,28,29]. Recent therapeutic strategies have focused on inducing biofilm dispersal, a process in which sessile bacteria transition to a planktonic state, thereby increasing their susceptibility to antimicrobial agents, through the use of chemical dispersal agents or degradation of the extracellular polymeric substance [13,30-33]

Previous studies have demonstrated that carbon dots, a class of spherical nanoparticles with diameters below 10 nm, can prevent or inhibit biofilm formation. For example, cellulase-derived CDs were shown to significantly reduce *P. aeruginosa* biofilm biomass. In addition, cur-CDs have been reported to exhibit antibiofilm activity against *Enterococcus faecium* [13,14,34]. Cur-CDs exert antibiofilm effects by disrupting bacterial membranes, inducing oxidative stress, inhibiting quorum sensing, and impairing EPS production, ultimately leading to reduced biofilm formation and destabilization of mature biofilms [13,14]. This study may provide one of the early investigations into the antibiofilm activity of curcumin-derived carbon dots against *P. aeruginosa* biofilms associated with urinary catheter surfaces.

This study demonstrates a concentration-dependent antibiofilm effect of cur-CDs against *Pseudomonas aeruginosa* biofilms formed on urinary catheter surfaces, as evidenced by significant reductions in both biofilm biomass (**Table 2**; p-value < 0.0001)) and viable bacterial counts (**Table 3**; p-value = 0.001). The combined assessment of optical density (OD) and colony-forming unit (CFU) enumeration provides a comprehensive evaluation of biofilm structural integrity and bacterial viability, which is essential for accurately characterizing antibiofilm efficacy [34]. Consistent with previous reports, the untreated control exhibited strong biofilm formation with high OD values and elevated CFU counts, reflecting the robust biofilm-forming capacity of *P. aeruginosa* on abiotic surfaces and its central role in catheter-associated urinary tract infections (CAUTI) [13,22]. Biofilm-embedded *P. aeruginosa* is known to exhibit increased tolerance to antimicrobial agents and host defences, underscoring the clinical relevance of targeting both biofilm biomass and viable cells [13].

At low cur-CDs concentrations (5 and 10 µg/mL), biofilm biomass remained classified as strong, and CFU analysis showed high number of bacterial colonies growth. These findings indicate that subinhibitory concentrations of cur-CDs are insufficient to suppress bacterial proliferation or disrupt the extracellular polymeric substance matrix. Similar observations have been reported for other nanoparticle-based and phytochemical antibiofilm agents, where inadequate dosing results in minimal biofilm disruption [13,14]. A transitional antibiofilm effect was observed at intermediate concentrations. At 20 µg/mL, cur-CDs significantly reduced CFU counts compared with the untreated group, suggesting impaired bacterial viability within the biofilm. However, OD measurements at this concentration displayed substantial variability, indicating heterogeneous effects on biofilm biomass. At higher concentrations (30 - 50 µg/mL), cur-CDs exerted pronounced antibiofilm activity. Biomass formation decreased from moderate to weak, accompanied by a marked and statistically significant reduction in CFU counts, with the lowest bacterial burden observed at 50 µg/mL.

Previous studies have reported that CDs synthesized from citric acid–curcumin [34] and aminoguanidine [35] may disrupt *P. aeruginosa* cell membranes through electrostatic interactions, thereby suppressing biofilm formation. Hydrophobic interactions may also contribute to membrane disruption. In addition, ROS generated following cur-CD treatment has been suggested to interfere with quorum sensing and downregulate biofilm-related gene expression, potentially inhibiting biofilm maturation and maintenance [13]. However, the precise mechanism by which cur-CDs damage the *P. aeruginosa* cell wall and inhibit biofilm biomass production, particularly in this study, remains unclear and requires further investigation. Furthermore, the effects of cur-CDs on the expression of biofilm-associated genes have not yet been fully elucidated. Based on these findings, we hypothesize that the dual reduction in biofilm biomass and viable bacterial load observed in this study may have potential clinical relevance for CAUTI prevention

and management, as effective control of biofilm-associated infections likely requires both eradication of biofilm-embedded bacteria and disruption of the protective biofilm matrix that contributes to bacterial persistence and recurrence.

The cytotoxicity assay of cur-CDs used in this study had been performed and reported in a prior publication. The results showed strong protective effects of cur-CDs, maintaining 100% cell viability at a concentration as low as 4 μg/mL, suggesting biocompatibility and biological effectiveness [19]. The findings of this study suggest that cur-CDs hold promise as a novel antibiofilm strategy, potentially applicable as a catheter surface coating or adjunctive intervention to limit *P. aeruginosa* colonization and biofilm development. Further *in vivo* studies and biocompatibility assessments are warranted to translate these in vitro findings into clinical application.

This study has several limitations that should be considered when interpreting the findings. First, the experiments were conducted entirely *in vitro* using a single reference strain (*Pseudomonas aeruginosa* ATCC 9027). While this model allows controlled evaluation of antibiofilm activity, it may not fully represent the heterogeneity, virulence, and antimicrobial tolerance observed among clinical *P. aeruginosa* isolates recovered from catheter-associated urinary tract infections. Future studies should include multiple clinical strains to improve generalizability. Second, biofilm formation was assessed on catheter pieces under static conditions, which do not replicate the dynamic urinary flow, shear stress, and physicochemical environment present in the human urinary tract. These factors are known to influence biofilm architecture, maturation, and antimicrobial susceptibility. Therefore, the antibiofilm efficacy of cur-CDs observed in this study may differ under physiologically relevant flow conditions. Third, although reductions in biofilm biomass and viable bacterial counts were demonstrated, the precise molecular mechanisms underlying the antibiofilm activity of cur-CDs were not directly investigated. Parameters such as quorum sensing inhibition, extracellular polymeric substance degradation, reactive oxygen species generation, and membrane integrity were not evaluated and warrant further mechanistic studies. Despite these limitations, this study provides important preliminary evidence supporting the potential of cur-CDs as an antibiofilm agent against *P. aeruginosa* on urinary catheter surfaces and lays the groundwork for future *in vivo* and translational investigations.

Conclusions

It is concluded that cur-CDs effectively inhibit *P. aeruginosa* biofilm formation on urinary catheter surfaces in a concentration-dependent manner, reducing both biofilm biomass and viable bacterial counts. These findings highlight the potential of cur-CDs as a promising antibiofilm strategy for mitigating catheter-associated urinary tract infections.

Acknowledgements

We are thankful to Wisnu Barlianto, the Dean of the Faculty of Medicine, Universitas Brawijaya, Malang, Indonesia, and Yuanita Mulyastuti, the Head of the Laboratory of Microbiology, Faculty of Medicine, Universitas Brawijaya, Malang, Indonesia, who facilitated our study. The excellent technical assistance of Ali Sabet is gratefully acknowledged. We are thankful to professor Yatim L Ni'mah for her valuable support in the FESEM examination process at Institut Teknologi Sepuluh Nopember, Surabaya, Indonesia.

Declaration of Generative AI in Scientific Writing

The authors acknowledge the use of generative AI tools (ChatGPT by OpenAI) in the preparation of graphical abstract. No content generation or data interpretation was performed by AI. The authors take full responsibility for the content and conclusions of this work

CRediT author statement

Dewi Santosaningsih: Conceptualization; Methodology; Validation; Writing - Original draft preparation; Supervision; Project administration. **Keneysha Naomi Mataniari**: Formal analysis; Investigation, Visualization. **Dian Nugrahenny**: Methodology; Validation; Writing - Original draft preparation; Supervision. **Azzania Fibriani**: Investigation; Resources; Supervision. **Arum Sinda Santika**: Formal analysis; Investigation, Visualization. **Fitri Aulia Permatasari**: Investigation; Resources;

Supervision; Writing - Original draft preparation. **Ferry Iskandar**: Resources; Supervision.

References

[1] H Rubi, G Mudey and R Kunjalwar. Catheter-associated urinary tract infection (CAUTI). *Cureus* 2022; **14(10)**, e30385.

[2] NA Obaid, SA Abuhussain, KK Mulibari, F Alshanqiti, SA Malibari, SS Althobaiti, M Alansari, E Muneef, L Almatrafi, A Alqarzi, N Alotaibi, AM Mostafa and A Hagag. Antimicrobial-resistant pathogens related to catheter-associated urinary tract infections in intensive care units: A multi-center retrospective study in the western region of Saudi Arabia. *Clinical Epidemiology and Global Health* 2023; **21**, 101291.

[3] World Health Organization. *Global report on infection prevention and control 2024*. World Health Organization, Geneva, Switzerland, 2024.

[4] C Suetens, T Karki and D Plachouras. *Point prevalence survey of healthcare associated infections and antimicrobial use in European acute care hospitals 2022-2023*. ECDC Surveillance, Stockholm, Sweden, 2024.

[5] ML Ling, P Ching, A Apisarnthanarak, N Jaggi, G Harrington and SM Fong. APSIC guide for prevention of catheter associated urinary tract infections (CAUTIs). *Antimicrobial Resistance & Infection Control* 2023; **12(1)**, 52.

[6] N Bouhrour, PH Nibbering and F Bendali. Medical device-associated biofilm infections and multidrug-resistant pathogens. *Pathogens* 2023; **13(5)**, 393.

[7] GT Werneburg. Catheter-associated urinary tract infections: Current challenges and future prospects. *Research and Reports in Urology* 2022; **14**, 109-133.

[8] AA Gheorghita, DJ Wozniak, MR Parsek and PL Howell. *Pseudomonas aeruginosa* biofilm exopolysaccharides: Assembly, function, and degradation. *FEMS Microbiology Reviews* 2023; **47(6)**, fuad060.

[9] FF Tuon, LR Dantas, PH Suss and VSR Ribeiro. Pathogenesis of the *Pseudomonas aeruginosa* biofilm: A review. *Pathogens* 2022; **11(3)**, 300.

[10] EN Sholikhah. Indonesian medicinal plants as sources of secondary metabolites for pharmaceutical industry. *Journal of Medical Sciences* 2016; **48(4)**, 226-239.

[11] ME Abd El-Hack, MT El-Saadony, AA Swelum, M Arif, MMA Ghanima, M Shukry, A Noreldin, AE Taha and KA El-Tarabily. Curcumin, the active substance of turmeric: Its effects on health and ways to improve its bioavailability. *Journal of the Science of Food and Agriculture* 2021; **101(14)**, 5747-5762.

[12] S Shome, AD Talukdar and H Upadhyaya. Antibacterial activity of curcumin and its essential nanoformulations against some clinically important bacterial pathogens: A comprehensive review. *Biotechnology and Applied Biochemistry* 2022; **69(6)**, 2357-2386.

[13] V Sawant, H Faleke, B Bhattarai, S Strickland, D Pappas and GF Christopher. Evaluating antibiofilm efficacy of carbon dots against *Pseudomonas aeruginosa* based on precursor molecule selection. *Colloids and Surfaces B: Biointerfaces* 2025; **254**, 114811.

[14] JK Trigo-Gutierrez, Y Vega-Chacón, AB Soares and EGDO Mima. Antimicrobial activity of curcumin in nanoformulations: A comprehensive review. *International Journal of Molecular Sciences* 2021; **22(13)**, 7130.

[15] MH Sadaqat, AM Mobarez and M Nikkhah. Curcumin carbon dots inhibit biofilm formation and expression of *esp* and *gelE* genes of *Enterococcus faecium*. *Microbial Pathogenesis* 2022; **173**, 105860.

[16] E Pericolini, B Colombari, G Ferretti, R Iseppi, A Ardizzoni, M Girardis, A Sala, S Peppoloni and E Blasi. Real-time monitoring of *Pseudomonas aeruginosa* biofilm formation on endotracheal tubes *in vitro*. *BMC Microbiology* 2018; **18(1)**, 84.

[17] AS Santika, FA Permatasari, B Khalfianisa, R Umami, BW Nuryadin, H Rachmawati and F Iskandar. N, O-functionalized curcumin-derived carbon dots for reactive oxygen species regulation: Mechanistic insights into biomedical applications. *ACS Applied Bio Materials* 2025; **8(6)**, 5194-5204.

[18] AS Santika, FA Permatasari, V Valencia, A Fibriani and F Iskandar. Toward a molecular-level

understanding of nitrogen functionalities in carbon dots for enhanced antibacterial activity and GSH detection. *Biomaterials Advances* 2025; **180**, 214592.

[19] A Fibriani, AAP Taharuddin, R Stephanie, N Yamahoki, J Laurelia, PH Wisnuwardhani, DF_Agustiyanti, M Angelina, Y Rubiyana, RA Ningrum, A Wardiana, F Iskandar, FA Permatasari and EA Giri-Rachman. Curcumin-derived carbon-dots as a potential COVID-19 antiviral drug. *Heliyon* 2023; **9(9)**, e20089.

[20] D Rachmawati, MZ Fahmi, MI Abdjan, EB Wasito, I Siswanto, N Mazlan, J Rohmah and A Baktir. *In vitro* assessment on designing novel antibiofilms of *Pseudomonas aeruginosa* using a computational approach. *Molecules* 2022; **27(24)**, 8935.

[21] S Swedan, Z Shubair and A Almaaytah. Synergism of cationic antimicrobial peptide WLBU2 with antibacterial agents against biofilms of multi-drug resistant *Acinetobacter baumannii* and *Klebsiella pneumoniae*. *Infection and Drug Resistance* 2019; **12**, 2019-2030.

[22] CR Thorn, A Wignall, Z Kopecki, A Kral, CA Prestidge and N Thomas. Liquid crystal nanoparticles enhance tobramycin efficacy in a murine model of *Pseudomonas aeruginosa* biofilm wound infection. *ACS Infectious Diseases* 2022; **8(4)**, 841-854.

[23] KD Mandakhalikar, JN Rahmat, E Chiong, KG Neoh, L Shen and PA Tambyah. Extraction and quantification of biofilm bacteria: Method optimized for urinary catheters. *Scientific Reports* 2018; **8(1)**, 8069.

[24] D Santosaningsih, Y Mulyastuti, S Poejiani, RF Putri, L Dewi, H Arifani, YL Ni'mah and A Baktir. The biofilm inhibition properties of glucosamine gold nanoparticles in combination with meropenem against *Pseudomonas aeruginosa* on the endotracheal tube: A model of biofilm-related ventilator-associated pneumonia. *Materials* 2024; **17(7)**, 1604.

[25] R Umami, FA Permatasari, S Fadilah, ECS Mahen, A Fibriani, T Hirano, T Ogi and F Iskandar. Rapid solvent-free synthesis of carbon dots with yellow to red emission for LED spectral conversion. *Diamond and Related Materials* 2025; **159(B)**, 112859.

[26] I Mong, V Ramoo, S Ponnampalavanar, MC Chong and WNFW Nawawi. Knowledge, attitude and practice in relation to catheter-associated urinary tract infection (CAUTI) prevention: A cross-sectional study. *Journal of Clinical Nursing* 2022; **31(1-2)**, 209-219.

[27] S Rajaramon, K Shanmugam, R Dandela and AP Solomon. Emerging evidence-based innovative approaches to control catheter-associated urinary tract infection: A review. *Frontiers in Cellular and Infection Microbiology* 2023; **13**, 1134433.

[28] W He, P Ma, L Li, D Wang, X Li, X Wen, Y Zuo, Q Guo, Y Zhang, R Cheng and Z Wang. Efficacy and safety of preventing catheter-associated urinary tract infection by inhibiting catheter bacterial biofilm formation: a multicenter randomized controlled trial. *Antimicrobial Resistance & Infection Control* 2024; **13**, 96.

[29] Y Su, JT Yrastorza, M Matis, J Cusick, S Zhao, G Wang and J Xie. Biofilms: Formation, research models, potential targets, and methods for prevention and treatment. *Advanced Science* 2022; **9(29)**, 2203291.

[30] E Silva, JA Teixeira, MO Pereira, CM Rocha and AM Sousa. Evolving biofilm inhibition and eradication in clinical settings through plant-based antibiofilm agents. *Phytomedicine* 2023; **119**, 154973.

[31] Q Zhang, Q Zong, X Feng, M Luo, W Sun and Y Zhai. Antibacterial and antifouling materials for urinary catheter coatings. *Acta Biomaterialia* 2025; **192**, 28-47.

[32] WK Redman, GS Welch, AC Williams, AJ Damron, WO Northcut and KP Rumbaugh. Efficacy and safety of biofilm dispersal by glycoside hydrolases in wounds. *Biofilm* 2021; **3**, 100061.

[33] Y Zou, Y Qu, Y Zhang and Q Yu. Multifunctional antibiofilm materials: Surface engineering and nanotherapeutic strategies for biofilm prevention and eradication. *Acta Biomaterialia* 2025; **203**, 155-180.

[34] F Lu, Y Ma, H Wang, M Zhang, B Wang, Y Zhang, H Huang, F Liao, Y Liu and Z Kang. Water-solvable carbon dots derived from

curcumin and citric acid with enhanced broad-spectrum antibacterial and antibiofilm activity. *Materials Today Communications* 2021; **26**, 102000.

[35] G Otis, S Bhattacharya, O Malka, S Kolusheva, P Bolel, A Porgador and R Jelinek. Chemical modification of carbon dots for selective labeling and growth inhibition of *Pseudomonas aeruginosa* by aminoguanidine carbon dots. *ACS Infectious Diseases* 2019; **5(2)**, 292-302.